ISSN 1392–1320 MATERIALS SCIENCE (MEDŽIAGOTYRA). Vol. 21, No. 1. 2015

Micro-structuring of Electrospun Mats Employing Femtosecond Laser

Erika ADOMAVIČIŪTĖ [1, 2 *], Tomas TAMULEVIČIUS [1], Linas ŠIMATONIS [1], Eglė FATARAITĖ-URBONIENĖ [1, 2], Edgaras STANKEVIČIUS [3], Sigitas TAMULEVIČIUS [1]

[1] *Institute of Materials Science, Kaunas University of Technology, K. Baršausko St. 59, LT-51423 Kaunas, Lithuania*
[2] *Department of Materials Engineering, Faculty of Mechanical Engineering and Design, Kaunas University of Technology, Studentų St. 56, LT-51424 Kaunas, Lithuania*
[3] *Institute of Physiology and Pharmacology, Medical Academy, Lithuanian University of Health Sciences, Mickevičiaus St. 9, LT-44307 Kaunas, Lithuania*

crossref http://dx.doi.org/10.5755/j01.ms.21.1.10249

Received 12 December 2014; accepted 23 March 2015

Electrospun mats from nano/micro-fibers with controlled porosity and pore shape may be ideal candidate for tissue engineering scaffolds. In this study three types of poly(vinyl alcohol) (PVA) mats of 41 μm – 66 μm thickness with different average nano/micro-fibers diameter of 100 nm – 200 nm were deposited on spunbond polypropylene (PP) filaments by electrospinning process. Controlled density porosity in the electrospun mats was introduced by Yb:KGW femtosecond laser micromachining system. The influence of electrospun mat microstructure, the distance between the adjacent laser ablation points, the number of femtosecond laser pulses on quality and structure of the laser irradiated holes were investigated. It was demonstrated that the quality of irradiated holes depends on the structure of electrospun mats (diameter of nano/micro-fibers, thickness of mats) and femtosecond laser processing parameters. Varying the distance between points of laser irradiation as well as number of applied femtosecond laser pulses it is possible to fabricate electrospun mats with increased porosity having extra pores of 22 μm – 36 μm in diameter.
Keywords: electrospinning, femtosecond laser, micro fabrication, scaffold.

1. INTRODUCTION

Electrospinning is a process for production of fine polymer fibres of submicron diameter. Electrospun nanofibers gained much attention due to their high surface area and pronounced micro and nano structural characteristics, which enable a myriad of advanced applications encompassing filtration devices, textile, electrical and optical components and sensors [1 – 3]. Electrospun nanofibers have been explored or developed as well for a variety of biomedical applications including medical implants, antimicrobial materials, wound dressing, dental materials, drug delivery vehicles, enzyme immobilization scaffolds, biomimetic actuators and sensors, scaffolds in tissue engineering [3]. Electrospinning presents several advantages with its comparative low cost and relatively high production rate. The morphology, fiber diameter and porosity of electrospun nanofibrous scaffolds can be controlled by varying parameters of electrospinning, such as applied electric field strength, spinneret diameter, distance between the spinneret and the collecting substrate, temperature, feeding rate, humidity, air speed, and properties of the solution or melt (such as the type of polymer, its molecular weight and concentration, surface tension, conductivity, viscosity, and temperature). Many polymers, both synthetic and natural, have been successfully electrospun into nanofibers, such as poly(ethylene terephthalate) (PET), polystyrene (PS), poly(vinyl chloride) (PVC), poly (*L*-lactide) (PLLA) and poly(ε-caprolactone) (PCL), among others [4, 5]. Electrospun poly(vinyl alcohol) (PVA) polymer has gained popularity as a scaffold supporting material for tissue engineering applications. PVA hydrogels have been used in a number of biomedical applications including soft contact lenses, cartilage implants, drug-delivery matrices, temporary skin covers or burn dressings and artificial organ [6]. This is because this polymer is non-toxic, non-carcinogenic, biocompatible, hydrophilic and demonstrates desirable physical properties such as rubbery or elastic nature and high degree of swelling in aqueous solutions [6 – 8].

While the nano/micro-fibrous scaffolds facilitate outstanding biological activities, due to their self-assembly nature there are some limitations, such as the difficulty to fabricate controllable three dimensional (3D) shapes and low controllability of porosity and pore shape [9]. In order to increase porosity of such materials various techniques were investigated to overcome this shortcoming, including incorporation of sacrificial fibers and porogens, modification of fiber diameter, post-processing by photopatterning or ultraviolet radiation treatment to increase pore size and overall porosity [5]. Smaller pore sizes increase the surface area of scaffolds and induce high cell attachment, while larger pore sizes induce easy migration of cells [9].

Laser micro-machining is a "lithography-free" structuring approach and therefore it is attractive for many biocompatible material direct processing applications. Due to small heat affected zone, ultrafast lasers are promising tools to rapidly process and create complex structures in electrospun mats [5]. In order to control cell behaviour and tissue development, laser ablation may be used to create microscale structures that control the size, shape and position of cell-extracellular matrix contacts [10]. It was demonstrated that it is possible to make homogeneous pore

*Corresponding author. Tel.: +370-655-41805; fax.: +370-37-353989
E-mail address: *erika.adomaviciute@ktu.lt* (E. Adomavičiūtė)

sizes [9] and complex true 3D structures [11] in electrospun PCL [4, 9, 11, 12] and PLLA [5] scaffold by femtosecond laser processing employing sample translation over focused laser beam [5, 9] or spatial light modulator based laser ablation [11], respectively. Typical reported laser processed structure sizes and forms in electrospun scaffolds (mats) varies from lines (of 1 μm – 15 μm widths and 15 μm – 110 μm depth) [11], to holes (of 50 μm – 436 μm diameters) [5, 9, 13] with 50 μm – 1000 μm center-to-center spacing and complex 2D drawings or even 3D pyramidal shapes [11]. Features produced by femtosecond laser usually have minimal melting of the remaining fiber at the edges of the ablation area [12]. Femtosecond lasers, as compared to nanosecond lasers, allow better control of laser power and enable to avoid fiber melting and consequently blockage of the porous structure [5]. Variety of lasers, laser irradiation conditions, applied materials used in the laser microfabrication are presented in Table 1 where summary of ultrafast laser processing conditions of different polymer electrospun mats from the related literature is presented.

Some of these microstructures found biological applications. E. g. to observe the feasibility of such femtosecond laser processed PCL [9] and PLLA [5] scaffolds with controlled pore size and density, they were seeded with osteoblast – like cells [9] and endothelial cell [5]. Based on the *in vitro* cell – culture observation, it was demonstrated that the electrospun 3D fibrous scaffolds with high pore structure can support significant cell adhesion and proliferation [9] and demonstrate significantly better endothelial cell in-growth and macrophage infiltration compared to the control scaffold *in vivo* [5].

The aim of this study is to investigate the effect of femtosecond laser irradiation on electrospun mats of different diameter PVA fibers as potential structures for biological application.

Table 1. Summary of ultrafast laser processing conditions of different polymer electrospun mats from related literature

Application, material	Electrospun mat thickness; fiber diameter	Laser wavelength (nm)	Pulse duration FWHM; Repetition rate (kHz);	Focusing conditions	Laser power, applied power	Pulse energy, applied pulse energy, number of pulses, fluence per pulse	Minimal ablated features, observed changes
Wettability modification of electrospun PCL fibers [10]	500 μm; 2.3 ±1.2 μm	775 nm ($Ti:Al_2O_3$)	150 fs; 2 kHz	Diffraction limited spot size1.3 μm defocusing experiment	0.5– 8 mW		Increased fiber dimension 3.1–9.4 μm
Wettability modification of electrospun PCL fibers [14]	500 μm; 2.8 ±1.8 μm	775 nm ($Ti:Al_2O_3$)	150 fs; 3 kHz	Diffraction limited spot size1.3 μm	1.5–12 mW		Increased fiber dimension 5.7–7.7 μm
3D PCL electrospun microstructures [11]	60.4–172.2 μm	800 nm ($Ti:Al_2O_3$)	130 fs; 1 kHz	Spatial light modulator in inverted microscope		1 mJ 1.25–4.75 μJ	Line 10 μm with 100 μm pitch lateral resolution 1–15 μm axial resolution 15–100 μm
Free standing PCL membranes [13]	100 μm; 0.4–0.9 μm (0.5 μm average)	800 nm ($Ti:Al_2O_3$)	65 fs; 1 kHz	Thin lens		1.5mJ, 0.17–0.75 J/cm^2	Hole diameter 600 μm
3D PCL scaffold [9]	0.5–2.5 μm (1.25 μm average)	800 nm ($Ti:Al_2O_3$)	35 fs; 1 kHz	Focused spot size 100 μm	4 W	3000 pulses	Fabricated pores size 189–380 μm
3D poly(L-lactide) PLLA scaffold for cells infiltration [5]	130–200 μm; 200 nm–3 μm	800 nm ($Ti:Al_2O_3$)	100 fs; 1 kHz	0.14 NA objective		7–70 μJ 1–10 pulses	Holes of 50–200 μm with pitch 20–200 μm
Improve pore size in PCL electrospun mat [4]	198 μm (540 nm average)	800 nm ($Ti:Al_2O_3$)	60-120 fs; 1 kHz	Fused silica lens of 500 mm focal length		100–600 μJ 1–5 pulses	Fabricated holes of 80–350 μm diameter
PCL scaffold for tissue engineering [12]	300 μm: 0.2–2 μm	800 nm ($Ti:Al_2O_3$)	150 fs; 2 kHz	Diffraction limited spot 2.6–6.4 μm;	1.6 W; 5–200 mW	0.75–1.5 μJ, 1–9.3 J/cm^2	Chanel width 10–250 μm, channel depth 50–250 μm
Polyethylene terephtalate (PET) scaffold [12]		1064 nm (Nd:YAG)	120 ns; 10 kHz	Diffraction limited spot 271 μm	50 W 3–10 W		

2. EXPERIMENTAL DETAILS

2.1. Electrospinning of PVA mats

Three different concentrations PVA (molecular weight ~ 61,000, Mowiol® 10-98, Sigma Aldrich) polymer solutions of different weight fractions 11 wt.%, 13 wt.% and 15 wt.% were prepared for electrospinning dissolving PVA granules in 80 ºC distilled water under magnetic stirring for four hours. The viscosity of different concentrations PVA solutions was measured by a viscometer – DV II+Pro (Brookfield Engineering Laboratories, Inc.). The obtained viscosities are summarized in Table 2.

Table 2. Average viscosities (η) of different concentration (C) PVA aqueous solutions with one standard deviation indicated in brackets. Shear rate 4.40 s^{-1}

C (wt.%)	11	13	15
η (mPa·s)	128 (27)	340 (45)	800 (24)

Mats of nano/micro-fibres from different PVA concentration solutions were deposited employing electrospinning machine Nanospider™ (Elmarco) on support material spunbond from polypropylene (PP) filaments (see Fig. 1).

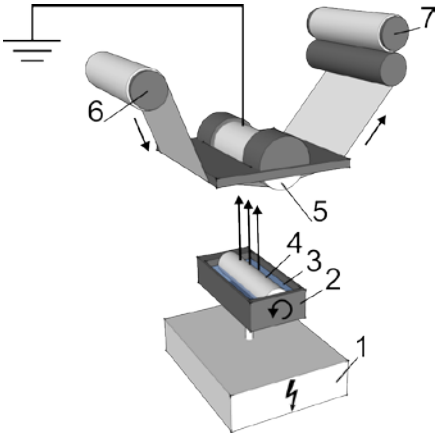

Fig. 1. Principal scheme of the electrospinning equipment – Nanospider™ (Elmarco): 1 – power supply with positive potential 0 kV – 75 kV, 2 – tray with polymer solution, 3 – polymer solution, 4 – rotating electrode with tines, 5 – grounded electrode, 6 – roller of support material spunbond from PP filaments, 7 – roller of support material spunbond from PP filaments with electrospun mat from nano/micro-fibers. Arrows indicate motion of polymer, substrate material and electrode

A nonwoven mat from nano/micro-fibers was formed at room temperature (t = 20 °C ±2 °C, air humidity γ = 44 % ±4 %), applying 70 kV voltage, the distance between electrodes was 13 cm, electrode spinning speed 5 rpm, durations of deposition process 6 min, mat thickness 41 µm – 66 µm.

2.2. Femtosecond laser micro-structuring of electrospun PVA mats

Femtosecond laser micro-structuring of electrospun PVA mat was performed employing FemtoLab micromachining system (Altechna R&D) and femtosecond (230 fs) 1030 nm wavelength Yb:KGW laser Pharos (04-500-PP, Light Conversion). The laser beam with quality of M^2=1.1 and diameter of 2.5 mm was focused with N.A. = 0.42 mm and 4 mm focal length 50× objective lens (Plan Apo NIR Infinity-Corrected, Mitutoyo). Micro-structuring was performed using 20 kHz pulse repetition rate and 0.47 W average laser power. Laser power was set using computer controlled attenuator Watt Pillot (Atlechna) measured with a power meter Nova II and thermal sensor 3A (Ophir). Five "Five by five" hole arrays with different adjacent point distances (50 µm – 90 µm with 10 µm step) were ablated employing XYZ translation stage (ANT130-160-XY, ANT130-5-V, Aerotech) and nonlinearly increasing number of pulses (26 – 7796 pulses) employing synchronized laser triggering from controlling software (SCA, Altechna R&D). The principle scheme is depicted in Fig. 2.

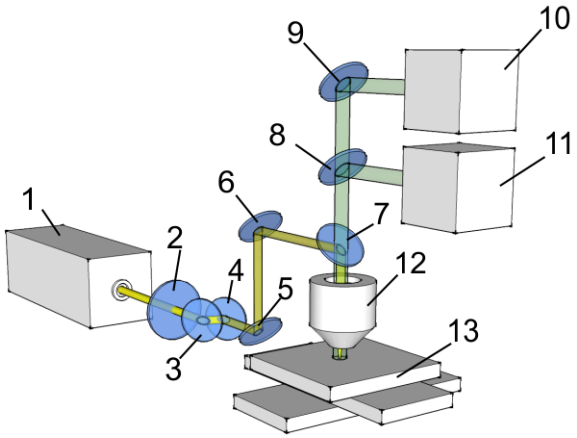

Fig. 2. Principal scheme of ultrafast laser micro-structuring system FemtoLab. 1 – femtosecond laser Pharos, 2 – λ/2 wave plate, 3, 4 – Brewster angle polarisers (2 – 4 – attenuator), 5 – 9 – dichroic mirrors, 10 – CCD camera, 11 – LED illumination, 12 – objective, 13 – XYZ stage

Table 3. Parameters of femtosecond laser micro-structuring

Average power (W)	0.47
Pulse temporal width (FWHM, fs)	230
Pulse repetition rate (kHz)	20
Energy per pulse (µJ)	23.6
Effective focal spot area (cm^2)	$5.07 \cdot 10^{-8}$
Peak power (W)	$1.02 \cdot 10^{8}$
Fluence per pulse (J/cm^2)	465
Intensity (W/cm^2)	$2.02 \cdot 10^{15}$
Number of applied pulses	26, 56, 236, 1316, 7796

Calculated diffraction limited focus spot of 2.54 µm was used for fluence per pulse (laser pulse energy/effective focal spot area) and intensity (laser peak power/effective focal spot area), where peak power (laser pulse energy/pulse duration), values estimation. Laser processing conditions are summarized in Table 3.

2.3. Scanning electron microscopy analysis

The structure and thickness of virgin and laser micro-structured electrospun PVA mats was analysed using a

field emission scanning electron microscope (SEM) Quanta 200 FEG (FEI) operating in a low vacuum mode. Electrospun PVA mats thickness was obtained from the razor blade cut cross sectional views in SEM, average of mat thickness was calculated from five measurements. The nano/micro-fibre diameter distribution and diameters of laser ablated holes were evaluated from the SEM micrographs employing an image analysis system LUCIA Image Version 5.0 (Laboratory Imaging).

2.4. Optical transmittance measurements

Electrospun mat transmittance in the near infrared range covering laser wavelength used in the microfabrication was obtained with a Fourier transform infrared (FT-IR) spectrometer VERTEX 70 (Bruker) employing a resolution of 2 cm^{-1} and 50 times averaging.

3. RESULTS AND DISCUSSION

SEM micrographs of the electrospun mats produced from different PVA concentration solutions are depicted in Fig. 3. One can see that the mats consist of uniform nano/micro-fibers. Mats obtained from the lowest concentration PVA solution (see Table 2, Fig. 3, a) besides nano/micro-fiber formation, demonstrate formation of embedded PVA beads with sub-micrometer linear dimensions.

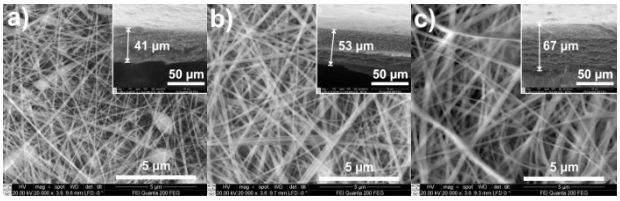

Fig. 3. The SEM micrographs of electrospun PVA mat structure (scale bar 5 µm) deposited from different PVA concentration solutions (also different resulting viscosities): a – 11 wt.%; b – 13 wt.%; c – 15 wt.%. The inset demonstrates SEM micrographs of electrospun mats cross-sections, arrows indicate thickness (scale bar 50 µm). Average of thickness: a – 41.3 µm ±1.6 µm; b – 53.3 µm ±3.4 µm; c – 66.7 µm ±1.3 µm

Fig. 4 presents nano/micro-fiber diameter distribution in the mats deposited from different concentration PVA solutions. The distributions were obtained analysing the SEM micrographs (see Fig. 3) with the image processing software. From Fig. 4 one can see that the lowest PVA viscosity (or smallest PVA concentration, 11 wt.%) provides fibers with the smaller diameter, i. e. 78 % of fibers demonstrate diameters up to 150 nm. In the case of higher PVA concentrations, i. e. 13 wt.% and 15 wt.%, only 48 % and 26 % of fibers demonstrate diameter up to 150 nm respectively. Increase of the average nano/micro-fiber diameter with increasing viscosity (and at the same time concentration of the polymer solutions) is in agreement with [15, 16].

Series of the focused femtosecond laser beam ablation experiments with different pulse numbers per point and different distances between the points were carried out to characterize the laser irradiation effects on the electrospun mats produced from different PVA concentration solutions. SEM micrographs of the electrospun mats after the micro-structuring with femtosecond laser under different conditions (see Table 4) are summarized in Fig. 5.

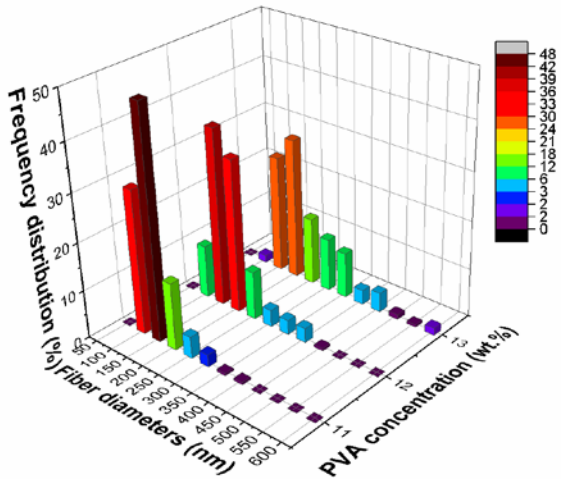

Fig. 4. Nano/micro-fiber diameter distribution of electrospun PVA mat deposited from three different concentration (11 wt.%, 13 wt.% and 15 wt.%) solutions

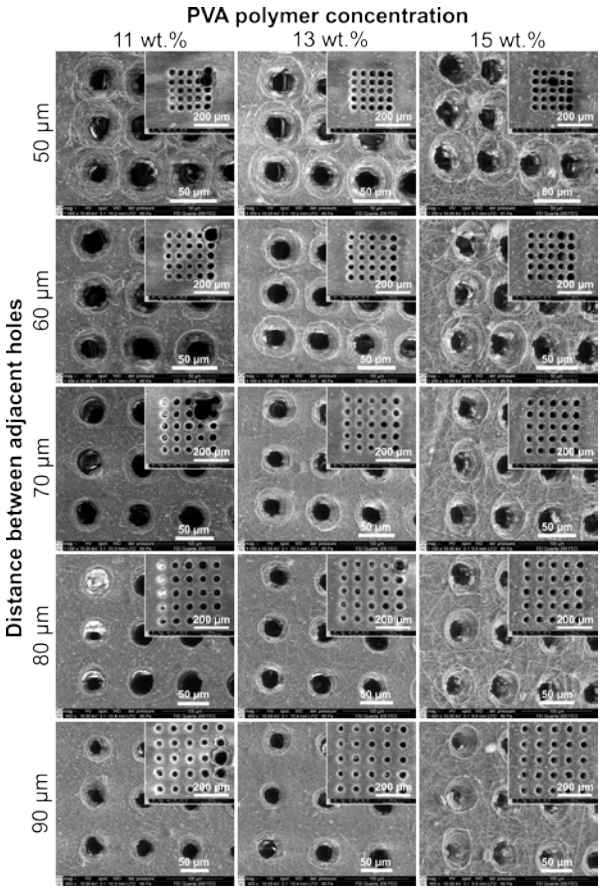

Fig. 5. SEM micrographs of the femtosecond laser micro-machined electrospun PVA mats deposited from different concentrations PVA solutions (11 wt.%, 13 wt.%, 15 wt.%). The distance between two adjacent holes increases from 50 µm to 90 µm with 10 µm steps. In each separate micrograph number of pulses used to produce micro-holes increases from 26 to 7796 from left to right (see Table 3 for more details). All five lines in each micrograph correspond to the identical laser processing conditions. Scale bar 50 µm. The inset demonstrates the whole five by five hole array in one micrograph, the scale bar is 200 µm

From Fig. 5 one can see that the biggest amount of defects (change of shape of the hole, overlapping of multiple holes) was obtained in the electrospun mat deposited from the lowest concentration PVA solution (11 wt.%). This fact could be explained by the structure of the sample, i. e. the fibers in such mats possess smallest diameters as seen from Fig. 4. It should be noted as well that in few cases, when the highest number of pulses (7796) was applied, the defects covering several adjacent holes, rather than the separate symmetrical holes, were obtained (see Fig. 5, 11 wt.%, 70 μm). Due to huge number of such defects the PVA mat electrospun from the lowest concentration solution (11 wt.%) was eliminated from the further hole diameter analysis. The influence of number of applied pulses and distance between the adjacent points during the laser irradiation on dimension of the holes are summarized in Table 4. The hole diameter in mats electrospun from two different concentration PVA solutions versus number of femtosecond laser pulses are depicted in Fig. 6.

From Table 4 and Fig. 6 one can see that the diameter of holes increases with the increase of applied number of pulses for both PVA concentrations. When the number of pulses increased from 26 to 7793 the diameter of holes increased approximately by 30 % in case of PVA mat with 13 wt.% and about 20 % for 15 wt.%. Comparing dimensions of the laser holes on PVA mat deposited from different concentration solutions, one can see that for the used range of PVA polymer concentrations it does not have significant influence on the diameter of femtosecond laser ablated holes. It is in agreement with [4] where hole diameter saturation was observed after certain number of pulses and it was valid for range of pulse energies, while it is in contrary to the observation described in [9] where thousands of pulses were applied and constant hole widening was observed. It should be mentioned that quite different optical setups and laser parameters as well as nano/micro-fiber diameter distributions and mat materials were used among the cited authors (Table 1) and in the current work.

It should be noted as well that changes in the number of pulses applied brings not only to the changes of the diameter of the holes but to the changes of interface in the vicinity of the hole too. Closer look at the laser ablated holes edges (see Fig. 7) reveals differences of the laser affected areas. One can see that besides the number of pulses these changes are also sensitive to the distance between the adjacent holes as well as to the used PVA polymer solution concentration during electrospinning of the mat. According to Fig. 7, in the vicinity of the hole, fiber microstructure and density of the material changes. The lower distance between the holes - the less unaffected area is left. The values of unaffected inter hole distances between two lines of holes obtained with 26, 58, 236 pulses are summarized in Table 5. It is in agreement with [10] where changes of the fiber diameter were observed. Melting of the mat and coverage of internal surface of the hole with molten material was reported as well in [13] where tens of micrometers wide laser affected – melted zones were observed.

Table 4. Average hole diameters with one standard deviation indicated in brackets of the laser processed electrospun mats obtained from the SEM micrographs

PVA concentration, *C* (wt.%)	Number of pulses	Average hole diameter (μm)				
		Distance between the adjacent points (μm)				
		50	60	70	80	90
13	26	23.1 (1.0)	23.1 (2.4)	22.4 (1.3)	26.1 (1.3)	25.0 (2.0)
	56	23.2 (2.6)	24.5 (3.8)	24.6 (1.3)	28.4 (1.1)	26.2 (2.7)
	236	29.6 (2.4)	26.0 (2.2)	24.6 (1.9)	27.9 (1.1)	28.8 (1.6)
	1316	31.2 (2.7)	28.2 (2.5)	28.6 (2.0)	28.9 (1.8)	30.4 (1.4)
	7796	32.8 (2.4)	35.7 (2.3)	32.8 (2.0)	36.6 (8.0)	35.2 (2.1)
15	26	27.2 (3.3)	26.9 (1.9)	28.5 (0.9)	27.2 (3.2)	24.3 (2.6)
	56	27.5 (1.9)	28.4 (2.8)	29.7 (1.7)	28.6 (1.6)	27.3 (2.1)
	236	31.9 (3.5)	29.3 (2.6)	32.3 (3.4)	25.6 (1.7)	26.4 (2.9)
	1316	29.9 (1.9)	34.1 (7.0)	32.7 (2.8)	30.4 (1.9)	31.8 (2.6)
	7796	35.4 (2.6)	36.6 (2.7)	33.8 (0.5)	31.7 (1.9)	33.8 (2.4)

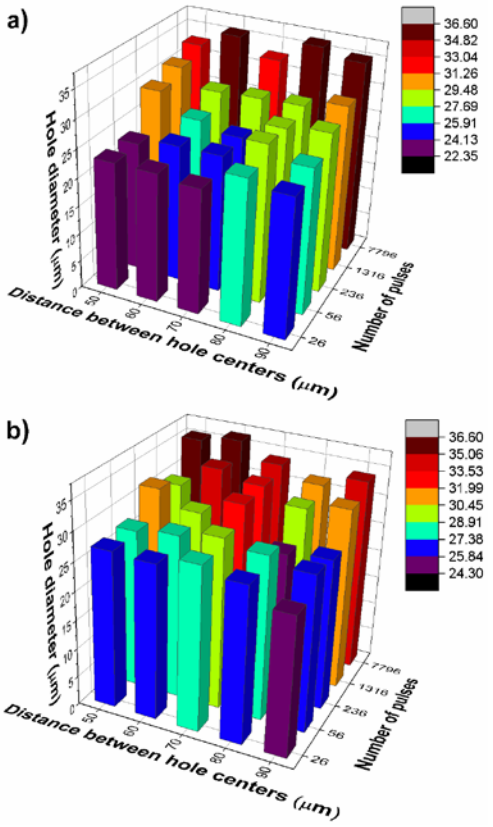

Fig. 6. The dependence of diameter of laser micro-structured holes upon applied number of pulses and distances between the adjacent holes for mats electrospun from two different concentrations PVA solutions: a – 13 wt.%, b – 15 wt.%

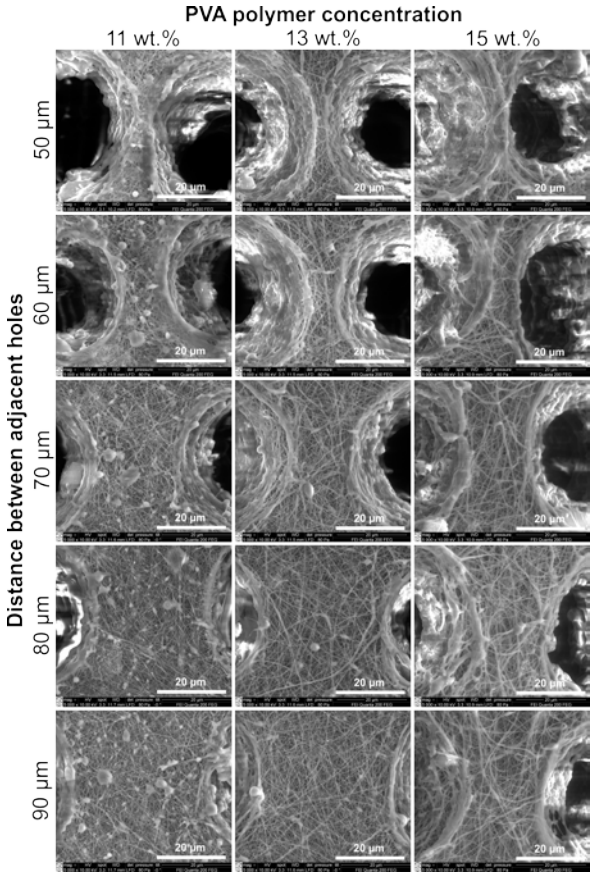

Fig. 7. SEM micrographs of the inter-hole areas of the femtosecond laser micro-machined (left hole 26 pulses, right hole 56 pulses) electrospun PVA mats obtained employing different viscosity (concentrations) PVA solutions and different hole density (distance between the adjacent points)

Table 5. The distance of not molten fiber area between the laser micro-machined holes (obtained from the SEM micrographs depicted in Fig. 5) with standard deviation indicated inside brackets obtained with 26, 56 and 236 pulses and different inter-hole distances (60 µm – 90 µm)

PVA concentration, *C* (wt.%)	Number of pulses	Distance of not molten area (µm)			
		Distance between the adjacent points (µm)			
		60	70	80	90
11	26	13.1 (1.4)	20.8 (1.1)	27.1 (1.5)	32.8 (7.7)
	58	11.0 (0.8)	19.5 (0.7)	30.8 (1.0)	39.5 (0.7)
	236	11.1 (0.4)	19.7 (7.4)	31.7 (1.9)	40.5 (2.4)
13	26	7.0 (0.8)	20.8 (4.2)	34.4 (4.2)	40.7 (2.1)
	56	8.3 (1.3)	21.3 (2.4)	30.0 (1.5)	39.6 (1.1)
	236	6.9 (2.9)	21.6 (1.3)	28.4 (1.8)	41.0 (1.7)
15	26	8.9 (3.2)	14.3 (0.9)	23.9 (2.5)	25.5 (1.4)
	56	10.5 (3.4)	15.7 (2.5)	27.2 (3.1)	33.6 (1.4)
	236	9.9 (1.7)	19.3 (1.8)	24.6 (2.3)	30.0 (2.0)

According to our results (Fig. 7), one can see that in the case of the smallest inter-hole distance (50 µm), the hole areas (areas of molten fibers after laser ablation) almost reach each other. The linear dimensions of these affected areas are sensitive to the distance between the neighbouring holes and increasing this distance allows preserving structure of unaffected electrospun fibers. E. g. for 13 wt.% PVA mat changing the distance from 60 µm to 90 µm allows to increase the unaffected area with the dimensions from 7.0 µm to 41.0 µm under employed laser processing conditions (see Table 5). Linear dimensions of the unaffected areas are also sensitive to the PVA concentration used during the electrospinning and fiber size of the mat indicating importance of the density of material in the heat conductivity and melting processes taking place during laser ablation [12]. Dependence of the heat unaffected area width on the hole density holds for low as well as for high number of applied pulses and for all the investigated densities of mat. Parameters describing mat structure next to the hole's interface for the different concentration solution PVA mats ablated with 25 and 7796 pulses are summarized in Fig. 8. One can see that the heat affected zone is smaller for mats with thicker fibers (highest PVA concentration) and biggest for the smallest fibers (smallest PVA concentration).

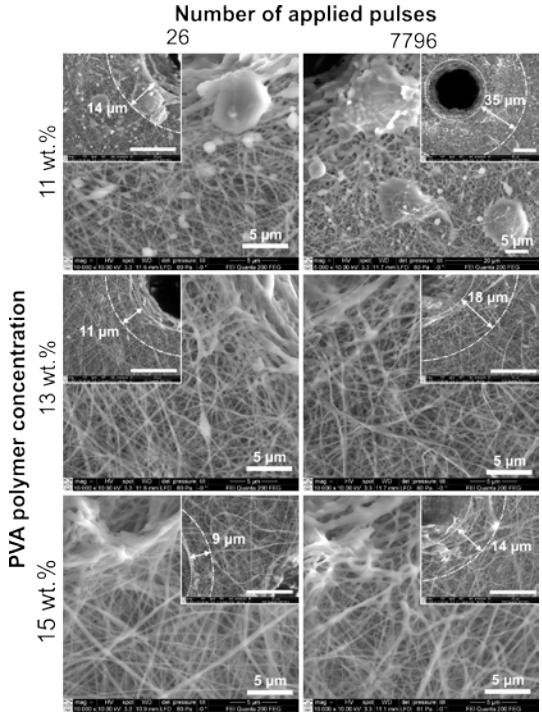

Fig. 8. SEM micrographs of femtosecond laser micro-machined electrospun next to the holes obtained after 25 and 7796 pulses (distance between holes 90 µm) for three different PVA concentrations. Scale bar 5 µm. Inset depicts heat affected zone indicated by arrow between two concentric rings, scale bar 20 µm

It should be noted that the heat affected zones indicated in Fig. 8 (i. e. 9 µm – 35 µm) as well as produced holes (22 µm – 37 µm) were much wider than the diffraction limited focal spot size used in the experiment. Similar situation was reported in [12], where diameter of the ablated structures was at least five time wider than diameter of the focused laser beam. Even wider heat

affected zones, were described in [13] where average width of the modified zone of 40 μm to 60 μm was observed next to the holes and lines ablated under conditions summarized in Table 1.

Fig. 9 illustrates structure of the internal surface of the laser ablated hole. It is well seen that fibers on the surface of electrospun mat were melt, but did not form a continuous film and still have the pores, which is very important for tissue scaffolds. Similar porous/melted hole edges were described in [4, 9, 12] but entirely different situation is described in [13] where porosity around the holes of the PCL mesh was lost. These differences could be explained in terms of pulse energies applied in ablation experiments, for more details see Table 1.

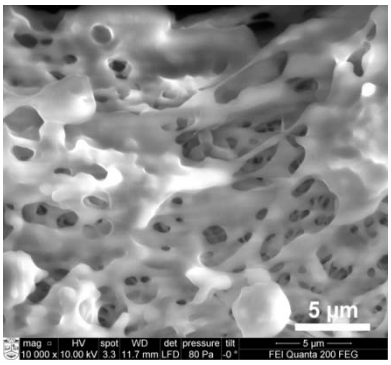

Fig. 9. SEM micrograph of the internal hole surface of femtosecond laser micro-machined (7795 pulses) electrospun PVA mat (11 wt.%). Scale bar 5 μm

Optical transmittance of the PVA mats in the NIR wavelength range close to the wavelengths applied for the ablations varies in the range of 15 % – 35 % (see Fig. 10). Differences in the transmittance could be related to the thickness of the electrospun mats, i. e. mat electrospun from i. e. 11 wt.% PVA concentration is the thinnest while – from 15 wt.% is the thickest (see Fig. 3), and also to the volume density of the mat, i. e. fiber diameter distribution and microstructure (see Fig. 4). It is in agreement with [12] where similar transmittance values were obtained for the electrospun PCL mats. Moreover it was demonstrated that mat extinction coefficient is much larger than the solid material absorption coefficient, i. e. scattering rather than absorption is a dominant factor in the attenuation of laser radiation trough the mat [12].

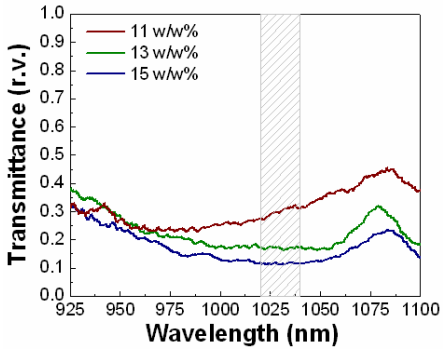

Fig. 10. FT-IR transmittance spectra in the vicinity of the laser wavelengths (dashed area) of electrospun mats from different concentration PVA solutions. Due to high noise 150 adjacent averaging smoothing was applied

In the current work the linear dimension and densities of holes in electrospun PVA mats are similar or smaller then reported in [13]. Based on the diffraction limited focused laser beam size one would expect smaller holes, but the effect of hole widening was also described in [12]. Wider features produced at high pulse energy may be attributed to melting and ablation of fibers beyond the radius of laser beam impingement by optical radiation from the plasma formed by interaction of laser radiation with fibers. Femtosecond impulses tend to melt fibers rather than ablate when fluence is below ablation threshold. Formation of plasma above solid surface being machined by femtosecond laser is a well-known limitation on the achieved precision of femtosecond laser ablation in ambient conditions. The plasma expands rapidly shortly after the femtosecond laser pulse and is observed to persist for many tens of nanoseconds [12]. Another possible reason for wide holes is variation of distance from focusing lens to the electrospun mat surface due to mat thinness variation or lens focus positioning errors [12].

The biggest differences of the mat used in the current experiment compared with other studies is the average nanofiber diameter which was smaller and therefore densities of the mat was higher compared with the results presented in [4, 9, 10,13, 14], where mostly micrometer range fibers were investigated. According to [11], nano/micro-fiber distribution of mats investigated in the current work is favourable for the femtosecond laser fabrication because in this process features smaller than certain size usually become limited by the fundamental characteristics of the mat (pore size and fiber diameter) and features smaller than 10 μm could be realized through careful adjustment of the exposure dose and focusing parameters only in tightly electrospun mats with smaller fiber diameters. So PVA mats deposited under conditions described in the current work are promising candidates for ablation of even smaller features employing high intensity femtosecond laser pulses [12].

It should be noted as well that the processes of microfabrication are dependent on the applied laser parameters. Until now most of the research in femtosecond laser microfabrication of electrospun mats was performed employing $Ti:Al_2O_3$ lasers at 800 nm wavelength, 1 kHz – 3 kHz repetition rates and 35 fs – 150 fs temporal width pulses (see Table 1). The laser employed in the current work enables much faster material processing because it supports up to 500 kHz pulse repetition rate, but at the same time the pulse width is longer (230 fs), therefore available pulse energies are smaller. The employed laser pulse width is still much shorter than typical ones in picosecond lasers. As a result heat diffusion due to thermal conduction is commensurately small, so that the processing materials can be handled more efficiently with little damage to the surrounding material and are adequate to avoid additional modification of the fibers [4, 9, 12].

All of these regularities of laser ablation of electrospun mats are extremely important in designing scaffolds for tissue engineering where the controlled diameter of pores is vitally necessary for the cell infiltration through the scaffolds. According to the presented results, employing femtosecond laser it is possible to form electrospun mats

with the controlled density and porosity, i. e. electrospun material with a diameter of pores 22 μm – 36 μm may be ideal candidate for the cell scaffolds application. To provide good quality of the microstructured electrospun mat it is necessary to choose the reasonable viscosity of polymer solution and femtosecond laser processing parameters.

4. CONCLUSIONS

It was demonstrated that electrospun poly(vinyl alcohol) (PVA) mat with well-defined holes size (with diameter from 22 μm to 36 μm) and with adjustable distance between the holes can be fabricated employing femtosecond laser micro-machining. The structure of electrospun mat (diameter of nano-/micro-fibers) has influence on the quality of femtosecond laser micro-structuring process. Higher PVA polymer concentrations (13 wt.% – 15 wt.%) mat with thicker fibers demonstrated less microstructuring defects, better quality of the holes and smaller heat affected zone. The diameter of holes depends on applied number or femtosecond laser pulses. The electrospun PVA fibers after femtosecond laser irradiation had tendency to melt, but the melted area of mat was still porous. Such microstrutured electrospun mat may be ideal candidate for cell scaffolds applications.

Acknowledgments

The authors would like to acknowledge financial support by the project VP1-3.1-ŠMM-10-V-02-029. Authors are also grateful to PhD student A. Čiegis for assistance with FT-IR measurements.

REFERENCES

1. **Krupa, A., Sobczyk, A. T., Jaworek, A.** Surface Properties of Plasma-modified Poly(vinylidene fluoride) and Poly (vinyl chloride) Nanofibres *Fibres and Textile in Eastern Europe* 22 2014: pp. 35 – 39.
2. **Amiri, P., Bahrami, S. H.** Electrospinning of Poly (acrylonitrile-acrylic acid)/β Cyclodextrin Nanofibers and Study of Their Molecular Filtration Characteristics *Fibres and Textile in Eastern Europe* 22 2014: pp. 14 – 21.
3. **Khadka, D. B., Haynie, D. T.** Protein- and Peptide-based Electrospun Nanofibers in Medical Biomaterials *Nanomedicine: Nanotechnology, Biology, and Medicine* 8 2012: pp. 1242 – 1262.
4. **Rebollar, E., Cordero, D., Martins, A., Chiussi, S., Reis, R. L., Neves, N. M., Leon, B.** Improvement of Electrospun Polymer Fiber Meshes Pore Size by Femtosecond Laser Irradiation *Applied Surface Science* 257 2011: pp. 4091 – 4095.
5. **Li-Ping Lee, B., Jeon, H., Wang, A., Yan, Z., Yu, J., Grigoropoulos, C., Li, S.** Femtosecond Laser Ablation Enhances Cell Infiltration into Three-Dimensional Electrospun Scaffolds *Acta Biomaterialia* 8 2012: pp. 2648 – 2658. http://dx.doi.org/10.1016/j.actbio.2012.04.023
6. **Asran, A. Sh., Henninh, S., Michler, G. H.** Polyvinyl alcohol – Collagen – Hydroxyapatite Biocomposite Nanofibrous Scaffold: Mimicking the Key Features of Natural Bone at the Nanoscale Level *Polymer* 51 2010: pp. 868 – 876.
7. **Algosseini, S. N., Moztarzadeh, F., Mozafari, M., Asgari, S., Dodel, M., Samadikuchaksaraei, A., Kargozar, S., Jalali, N.** Synthesis and Characterization of Electrospun Polyvinyl Alcohol Nanofibrous Scaffolds Modified by Blending with Chitosan for Neural Tissue Engineering *International Journal of Nanomedicine* 7 2012: pp. 25 – 34.
8. **Kim, C. H., Khil, M. S., Kim, H. Y., Lee, H. U., Jahng, K. Y.** An Improved Hydrophilicity via Electrospinning for Enhanced Cell Attachement and Proliferation *Journal of Biomedical Materials Research Part B: Applied Biomaterial* DOI 10.1002/jbmb
9. **Kim, M. S., Son, J. G., Lee, H., Hwang, H., Hyun Choi, C.** Highly Porous 3 D Nanofibrous Scaffolds Processed with an Electrospinning/Laser Process *Current Applied Physics* 14 2014: pp. 1 – 7. http://dx.doi.org/10.1016/j.cap.2013.10.008
10. **He, L., Chen, J., Farson, D. F., Lannutti, J. J., Rokhlin, S. I.** Wettability Modification of Electrospun Poly (ε-caprolactone) Fibers by Femtosecond Laser Irradiation in Different Gas Atmospheres *Applied Surface Science* 257 2011: pp. 3547 – 3553.
11. **Jenness, N. J., Wu, Y., Clark, R. L.** Fabrication of Three-dimensional Electrospun Microstructures Using Phase Modulated Femtosecond Laser Pulses *Materials Letters* 66 2012: pp. 360 – 363.
12. **Choi, H., Johnson, J. K., Nam, J., Farson, D. F., Lannutti, J.** Structuring Electrospun Polycaprolactone Nanofiber Tissue Scaffolds by Femtosecond Laser Ablation *Journal of Laser Applications* 19 (4) 2007: pp. 225 – 231.
13. **Wu, Y., Vorobyev, A. Y., Clark, R. L., Guo, Ch.** Femtosecond Laser Machining of Electrospun Membranes *Applied Surface Science* 257 2011: pp.2432 – 2435.
14. **He, L., Farson, D. F., Chen, J., Lannutti, J. J., Rokhlin, S. I.** Wettability Modification of Electrospun Poly (ε-caprolactone) Fiber by Femtosecond Laser Irradiation *Journal of Laser Applications* 2013. http://dx.doi.org/10.2351/1.476822
15. **Cramariuc, B., Cramariuc, R., Scarlet, R., Manea, L. R., Lupu, I. G., Cramariuc, O.** Fiber Diameter in Electrospinning Process *Journal of Electrostatics* 71 2013: pp.189 – 198.
16. **Heikkila, P., Harlin, A.** Parameter Study of Electrospinning of Polyamide 6 *European Polymer Journal* 44 2008: pp. 3067 – 3079. http://dx.doi.org/10.1016/j.eurpolymj.2008.06.032